# Study of Electronic Spectra of Free-Base Porphin and Mg-Porphin: Comprehensive Comparison of Variety of *Ab Initio*, DFT, and Semiempirical Methods

**JOSEF ŠEDA,[1] JAROSLAV V. BURDA,[1] JERZY LESZCZYNSKI[2]**
*[1]Department of Chemical Physics and Optics, Faculty of Mathematics and Physics,*
*Charles University, Ke Karlovu 3, 121 16 Prague 2, Czech Republic*
*[2]Department of Chemistry, Jackson State University, 1325 J.R. Lynch St.,*
*Jackson, Mississippi 39217-0510*

*Received 21 July 2004; Accepted 21 October 2004*
*DOI 10.1002/jcc.20164*

**Abstract:** SAC (symmetry adapted cluster)/SAC-CI and CASPT2 (multiconfigurational second-order perturbation theory) electron excitation spectra of free-base porphin and magnesium-porphin were determined using basis set functions augmented by both the polarization and diffuse functions—6-31+G(d). Such basis is recommended for correct description of the spectra because diffuse functions play fundamental roles in the formation of Rydberg MOs. The obtained results indicated that already the lowest roots in $A_u$, $B_{1u}$, $B_{2g}$, and $B_{3g}$ irreducible representations display Rydberg character. The calculated spectra are in a good agreement with both experimental and recently calculated electronic transitions. It is concluded that the SAC/SAC-CI level spectral lines are significantly affected by configuration selection when energy thresholds $5.0 \times 10^{-6}$ and $5.0 \times 10^{-7}$ a.u. are used for the determination of ground and excited state properties.

© 2004 Wiley Periodicals, Inc. J Comput Chem 26: 294–303, 2005

**Key words:** free-base porphin; magnesium-porphin; FBP; MgP; photosynthetic model; electron spectra calculations

## Introduction

Porphyrins play a key role in many important biological processes like oxygen absorption and transport, electron transport during the initial photochemical steps in photosynthesis, and so forth.[1] To clarify the mechanism of these reactions, the electronic properties of porphyrins have been extensively investigated.[2–9] Free-base porphin (FBP; Fig. 1) can be considered as a basic unit from which porphyrins are derived; various theoretical approaches were recently used to clarify its electronic structure and spectrum.

The metallo-porphins frequently participate in biological processes. Their central part is occupied by a divalent cation. In the case of magnesium porphin it is $Mg^{2+}$ ion (MgP; Fig. 1). The electronic and structural properties of various metallo-porphins are to some extent similar.[10]

Edwards *et al.*[11,12] performed the first extensive investigation on spectroscopic properties of porphyrins in vapor phase. Very weak so-called Q band exists in the visible region of the spectrum. The most intense absorption called B or Soret band occurs in the near-UV region. Two weaker and broad bands (N and L) and one intensive high-energy M band were detected in the UV region. A significant difference between metallo-porphins and free-base form is demonstrated in the splitting of the Q band due to the loss of square symmetry of the molecular structure. We are not aware of any experimental absorption spectrum of MgP in the vapor phase. The detected spectra of MgP derivatives [1,3,5,7-tetramethyl-2,4,6,8-tetraethylporphin-Mg (MgEthioP)[12] and 9,10,11,12-tetraphenylporphin-Mg (MgTPP)[11]] usually serve for the comparison with theoretical calculations.

In the beginning of 60's, Gouterman[13,14] introduced a four orbital model within the Hückel method and was able to reproduce basic spectral lines (Q and B) of porphyrins. Later, *ab initio* CI-Singles (CIS) method was presented and applied to the study of the FBP spectrum in Pople's group.[15] Nakatsuji *et al.* developed a high correlated SAC[16]/SAC-CI[17,18] method, and the calculations of electron transitions on FBP molecule performed using his approach were reported in ref. 19–21. The same quality of basis set (DZ) and thresholds were applied for calculation of the MgP

---

*Correspondence to:* J. Burda; e-mail: burda@karlov.mff.cuni.c2

Contract/grant sponsor: Grant Agency of Charles University

Contract/grant sponsor: NSF-CREST; Contract/grant number: HRD-0318519

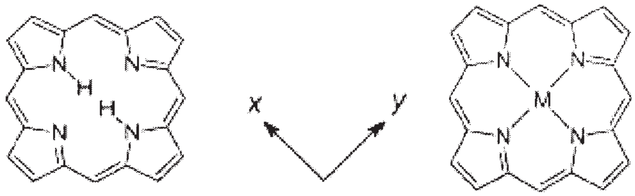

**Figure 1.** Free-base porphin and Mg-porphin together with standard orientation of the coordinate axes.

spectrum.[22] Simultaneously, another group of methods was introduced (STEOM-CC and STEOM-MP2) and used for the determination of electron spectra of FBP.[23,24] Configuration selection based on composite natural orbital method was applied in MRSD$\sigma\pi$CI calculation, which reproduced selected singlet and triplet states of FBP with high accuracy.[25] Another MRCI study of FBP spectra using RASSCF reference function was published recently by Werner's group.[26] Merchan *et al.*[27] published first multireference CASPT2 spectra calculations on FBP. Their selection of active orbitals was based on $\pi$-RASSCF calculation. Larger active spaces were used in later calculations on FBP[28] and MgP.[29] Hashimoto *et al.*[30] studied Q and B bands of FBP, MgP, ZnP, and their derivatives by the multireference Møller-Plesset perturbation theory with CASSCF reference functions. Recently, also a number of DFT-based calculations of excited state properties have been published. Time-dependent density functional theory (TDDFT) was used for the prediction of the electronic spectra of FBP[31–34] and MgP.[35] Multireference CI method with DFT reference function was applied to determine spectra of various porphyrins,[36] chlorophyll *a*, and pheophytin *a* models.[37]

In this article we present the results of a systematical study on electronic spectra of FBP and MgP. Various recently developed quantum chemical methods (CASPT2, SAC-CI, TDDFT, RPA, and CIS) were investigated and compared with the respect to their accuracy and efficiency for the spectra determination of more complex systems. All calculations were performed using basis set augmented by diffuse (s,p) and polarization (d) functions in order to reproduce experimentally observed transitions as close as possible (see also ref. 38).

## Computational Details

Optimizations of the ground state geometries of FBP and MgP was performed at the Hartree-Fock level with 6-31G(d) basis set, assuming $D_{2h}$ and $D_{4h}$ point group of symmetry, respectively. Because frozen resonance structures are preferred within this approximation, consideration of such symmetry restrictions is recommended.[3,39,40] Commonly used axes orientation was applied for the spectra transitions characterization: all the nitrogen atoms were positioned on the $x$- and $y$-axes and in the case of FBP the protonated nitrogens lay along the $x$-axis (cf. Fig. 1).

Pople's 6-31+G(d) basis set[41,42] was used for all the calculations of electron spectra. The basis set dependence was studied recently at CIS, RPA, TDDFT, and CASSCF levels.[38] Including some of these results we would like to present a systematical study of various methods (advantages and drawbacks) within a unified and reliable basis set. Also, the importance of electron correlation included in SAC/SAC-CI and CASPT2 methods for the ground and excited states is demonstrated in comparison with CIS, RPA, and TDDFT spectra from our previous work.[38]

In the SAC[16]/SAC-CI[17,18] calculations only inner core MOs were frozen. Energy thresholds of $5.0 \times 10^{-6}$ and $5.0 \times 10^{-7}$ a.u. were used in the configuration selection step for the energy determination of the ground and excited states, respectively. These thresholds are labeled as "LevelTwo" in the GAUSSIAN 03 program suite.[43] Previously published calculations[19,20,22] adopted a little worse threshold for the ground state ($1.0 \times 10^{-5}$ a.u.) as well as for the other than $\pi$-$\pi$* excitations ($1.0 \times 10^{-6}$ a.u.). Kitao *et al.*[21] presented a systematic study in the SAC-CI framework of theory and concluded that the results with the $1.0 \times 10^{-5}$ threshold value for the ground state and $5.0 \times 10^{-7}$ for the excited states are acceptable as far as the optically allowed excited states are computed. We were able to compute the lowest transitions using more accurate thresholds ($1.0 \times 10^{-6}$ and $1.0 \times 10^{-7}$ a.u., "LevelThree") applying the 6-31G basis set. Table 1 shows the dimensions of the linked terms before and after the selection.

The CASPT2 method, the second-order perturbation theory with multiconfigurational reference state,[26] was used to calculate

**Table 1.** Dimensions of the Linked Terms before and after the Selection in SAC/SAC-CI Spectra Calculations of FBP.[a]

| | 6-31+G(d) | LevelOne | LevelTwo | 6-31G | LevelOne | LevelTwo | LevelThree |
|---|---|---|---|---|---|---|---|
| SAC/Ag | 34031854 | 37295 | 105061 | 5920901 | 27850 | 69986 | 416844 |
| SAC-CI | | | | | | | |
| B2u | 34019122 | 99440 | 185281 | 5916092 | 30814 | 51241 | 129863 |
| B3u | 34019774 | 86701 | 161525 | 5916248 | 33104 | 56661 | 152200 |

[a]LevelOne: $1.0 \times 10^{-5}$ and $1.0 \times 10^{-6}$ a.u., LevelTwo: $5.0 \times 10^{-6}$ and $5.0 \times 10^{-7}$ a.u., LevelThree: $1.0 \times 10^{-6}$ and $1.0 \times 10^{-7}$ a.u. for the ground and excited states, respectively.

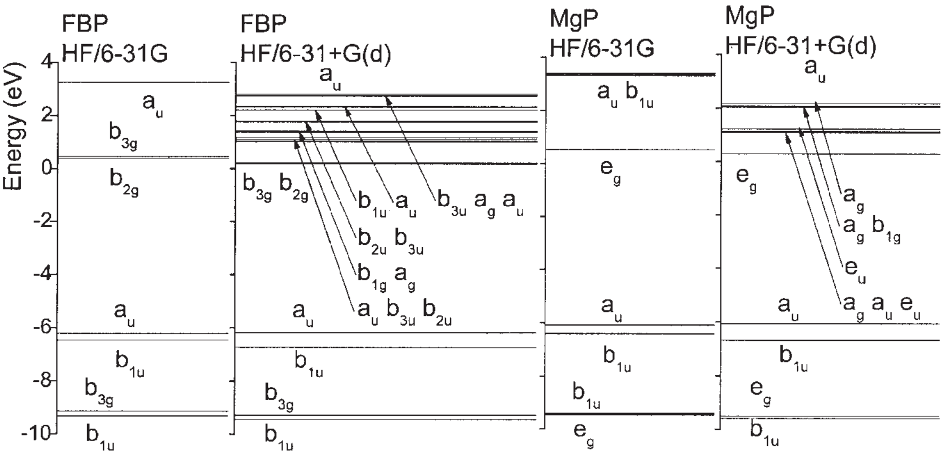

**Figure 2.** Comparison of energy of the most important orbitals calculated at HF level.

the electronic spectrum of FBP and MgP. The CASSCF optimized wave functions were used as reference functions for the inclusion of dynamic correlation effects. The transition dipole moments were determined using CASSCF state interaction (CASSI) method (cf. ref. 27 for more details). Because of technical reasons all calculations were carried out in the $D_{2h}$ symmetry. Level-shift of 0.4 a.u. was adopted in all calculations to get rid of difficulties with possible intruder-states (according to recommendation in ref. 29). Deterioration of the excitation energies was less than 0.2 eV in comparison with the nonshifted results (where available). An average CASSCF procedure was used for the lowest four excited states in the $B_{3u}$ and $B_{2u}$ irreducible representation. Ground state of $A_g$ symmetry was optimized individually.

The specifics of our calculations were based on the recommendations of the recently published investigations,[28,29] where active space (14/16) (the number of active orbitals/the number of active electrons) was used. Specifically, the three highest occupied and one lowest unoccupied orbital (4/6) from $B_{1u}$, irrep., (4/4) from both $B_{2g}$ and $B_{3g}$, and (2/2) from $A_u$ irreps were included. It should be emphasized that the three Rydberg type orbitals exist in this active space, in contrast to previous calculations where no diffuse functions were included in the AO basis set. The Gouterman's "4 orbital" active space (4/4) was also investigated for comparison.

The SAC/SAC-CI and CASPT2 level calculations were performed using GAUSSIAN 03 and Molcas-5[44] quantum chemistry software, respectively.

## Results and Discussion

### *FBP*

#### *Ground State Electronic Structure*

Ground state of FBP has a singlet electron configuration of the $D_{2h}$ group symmetry. It is comprised of the following representations: $20a_g^2\ 17b_{2u}^2\ 17b_{3u}^2\ 14b_{1g}^2\ 5b_{1u}^2\ 3b_{3g}^2\ 3b_{2g}^2\ 2a_u^2$. The presence of polarization functions in the basis set slightly affects the ordering of the lowest valence orbitals.[38] The application of diffuse functions allows describing Rydberg type orbitals, which are very low in energy. In our calculations the Rydberg-valence mixing was not observed (see also ref. 20). In Figure 2, energy levels of the most important MOs are compared. (Individual MOs are available upon request.)

#### *Spectra Calculations of Singlet States*

*SAC/SAC-CI.* The effect of configuration selection threshold was studied within 6-31G basis set. First we should mention the dependence of transition energy on the number of calculated spectral lines within a given irreducible representation. There is up to 0.12 eV difference when we compare calculations of two and three lowest transitions within $B_{2u}$ irrep. (irreducible representation of the $D_{2h}$ point group of symmetry) at LevelTwo configuration selection threshold level (compare in Table 2). A deeper insight into configuration selection is provided by Kitao.[21] However, further improvement of the quality of results was noticed after improving the level of calculations with configuration selection at LevelThree. The difference between spectral lines calculated at LevelTwo and LevelThree was up to 0.3 eV. Unfortunately, using 6-31+G(d) basis set it was not possible to calculate SAC/SAC-CI spectra with the most accurate configuration selection thresholds (LevelThree), thus LevelTwo was used for all calculations with this basis set instead (comparable thresholds were also used in ref. 19,20,22).

The lowest excitations ($1B_{3u}$ and $1B_{2u}$) correspond to $Q_x$ and $Q_y$ bands, and their energies are slightly below the experimental values[12] (by 0.2 and 0.3 eV, respectively). The electronic transitions from $2a_u$ to $4b_{3g}$ and from $5b_{1u}$ to $4b_{2g}$ are included in the $1B_{3u}$ excited state, and both contribute about 45%. The double excitations represent only about 8% contributions in the wave function expansion. Similarly, the first $B_{2u}$ excited state is mainly composed of $5b_{1u}$ to $4b_{3g}$ and $2a_u$ to $4b_{2g}$ electronic transitions. In the second lowest excited states ($2B_{3u}$ and $2B_{2u}$), transition from $4b_{1u}$ orbital is partially admixed to 4 orbital

**Table 2.** SAC-CI Calculated Spectra Lines where 4 (a), 3 (b), or 2 (c) Lowest Roots Were Calculated in Both $B_{3u}$ and $B_{2u}$ Irreps.[a]

| FBP | $1A_g$ | $1B_{3u}$ | $2B_{3u}$ | $3B_{3u}$ | $4B_{3u}$ | $1B_{2u}$ | $2B_{2u}$ | $3B_{2u}$ | $4B_{2u}$ | $1B_{1g}$ | $1B_{1u}$ | $1B_{2g}$ | $1B_{3g}$ | $1A_u$ |
|---|---|---|---|---|---|---|---|---|---|---|---|---|---|---|
| 6-31G/One/(a) | **4.48** | **1.86** | **3.72** | **4.35** | **5.11** | **2.35** | **3.84** | **4.55** | **5.07** | **4.47** | **4.54** | **4.25** | **3.93** | **4.31** |
| | | *0.00* | *1.23* | *0.74* | *0.39* | *0.00* | *1.71* | *0.23* | *0.31* | | *0.01* | | | |
| 6-31G/Two/(a) | **4.55** | **1.92** | **3.83** | **4.46** | **5.25** | **2.39** | **3.98** | **4.66** | **5.17** | **4.03** | **4.67** | **4.40** | **4.60** | **4.45** |
| | | *0.00* | *1.19* | *0.88* | *0.36* | *0.00* | *1.75* | *0.24* | *0.33* | | *0.01* | | | |
| 6-31G/Two/(b) | | **1.95** | **3.85** | **4.50** | | **2.40** | **4.00** | **4.71** | | | | | | |
| | | *0.00* | *1.19* | *1.08* | | *0.00* | *1.78* | *0.36* | | | | | | |
| 6-31G/Two/(c) | | **1.99** | **3.94** | | | **2.45** | **4.12** | | | | | | | |
| | | *0.00* | *1.55* | | | *0.01* | *2.14* | | | | | | | |
| 6-31G/Three/(c) | **4.60** | **2.13** | **4.14** | | | **2.55** | **4.37** | | | **4.20** | **4.94** | **4.77** | **4.89** | **4.78** |
| | | *0.00* | *1.39* | | | *0.01* | *2.23* | | | | *0.01* | | | |
| 6-31+G*/Two/(b) | **4.41** | **1.80** | **3.57** | **4.23** | | **2.13** | **3.67** | **4.34** | | **3.71** | **4.70** | **4.83** | **4.77** | **4.59** |
| | | *0.01* | *1.17* | *0.95* | | *0.00* | *1.64* | *0.35* | | | *0.01* | | | |

| MgP | $1A_g$ | $1E_u$ | $2E_u$ | $3E_u$ | $1B_{1g}$ | $1B_{1u}$ | $1E_g$ | $1E_g$ | $1A_u$ |
|---|---|---|---|---|---|---|---|---|---|
| 6-31G/Two/(b) | **4.56** | **1.96** | **3.70** | **4.25** | **4.50** | **5.13** | **4.82** | **4.82** | **5.25** |
| | | *0.00* | *1.74* | *0.03* | | *0.01* | | | |
| 6-31+G*/Two/(b) | **4.09** | **1.68** | **3.29** | **3.81** | **3.94** | **3.82** | **4.14** | **4.14** | **3.66** |
| | | *0.01* | *1.56* | *0.00* | | *0.00* | | | |

[a] **Bold** are transition energies (eV), italic are corresponding transition dipole moments (a.u.). Configuration selection thresholds: LevelOne: $1.0 \times 10^{-5}$ and $1.0 \times 10^{-6}$ a.u., LevelTwo: $5.0 \times 10^{-6}$ and $5.0 \times 10^{-7}$ a.u., LevelThree: $1.0 \times 10^{-6}$ and $1.0 \times 10^{-7}$ a.u. for the ground and excited states, respectively.

scheme (24% in $2B_{3u}$ and only ca. 7% in $2B_{2u}$). The $2B_{3u}$ and $2B_{2u}$ transitions correspond to quasidegenerate B band. The calculated energies are approximately 0.3 eV above experimental results. The excitations from the $4b_{1u}$ orbital provide the main contribution to the next excited states, $3B_{3u}$ and $3B_{2u}$ (63 and 78%, respectively). These excitations define the N band and their energies are estimated about 0.7 eV above the experiment. The first suggestion that also this line should be degenerated comes from the computational study of Roos's group performed at CAS-PT2 level,[27,28] and the same suggestion was later expressed by van Gisbergen based on his TDDFT study.[33] The calculated position of electron transitions can be seen in Figure 3.

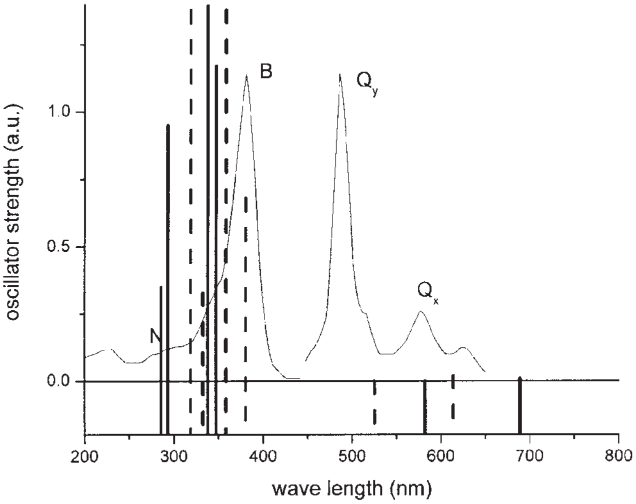

**Figure 3.** Comparison of calculated spectra of FBP with experimental data.[12] Solid lines represent SAC-CI determined transitions, dashed lines correspond to CASPT2 spectrum. Q band intensity is 10× enlarged.

**Table 3.** CASSCF Wave Function Composition for the Excited States of FBP and MgP.[a]

| State | Configuration | Weight (%) | State | Configuration | Weight (%) |
|---|---|---|---|---|---|
| FBP | — | — | $1B_{2u}$ | $5b_{1u}$:$4b_{3g}$ | 41 |
| $1B_{3u}$ | $2a_u$:$4b_{3g}$ | 43 | | $2a_u$:$4b_{2g}$ | 34 |
| | $5b_{1u}$:$4b_{2g}$ | 36 | $2B_{2u}$ | $3b_{1u}$:$4b_{3g}$ | 26 |
| $2B_{3u}$ | $2a_u$:$4b_{3g}$ | 31 | | $2a_u$:$4b_{2g}$ | 23 |
| | $5b_{1u}$:$4b_{2g}$ | 29 | | $5b_{1u}$:$4b_{3g}$ | 15 |
| | $3b_{1u}$:$4b_{2g}$ | 12 | | $4b_{1u}$:$4b_{3g}$ | 5 |
| $3B_{3u}$ | $4b_{1u}$:$4b_{2g}$ | 55 | $3B_{2u}$ | $3b_{1u}$:$4b_{3g}$ | 41 |
| | $3b_{1u}$:$4b_{2g}$ | 9 | | $5b_{1u}$:$4b_{3g}$ | 15 |
| $4B_{3u}$ | $3b_{1u}$:$4b_{2g}$ | 39 | | $2a_u$:$4b_{2g}$ | 12 |
| | $2a_u$:$4b_{3g}$ | 13 | $4B_{2u}$ | $4b_{1u}$:$4b_{3g}$ | 36 |
| | $5b_{1u}$:$4b_{2g}$ | 11 | | $2a_u$,$3b_{3g}$:$4b_{2g}$,$4b_{3g}$ | 14 |
| | $4b_{1u}$:$4b_{2g}$ | 6 | | $2a_u$:$4b_{2g}$ | 7 |
| MgP | — | — | $3E_u$ | $5b_{1u}$:$4e_g$ | 49 |
| $1E_u$ | $2a_u$:$4e_g$ | 42 | | $6b_{1u}$:$4e_g$ | 11 |
| | $6b_{1u}$:$4e_g$ | 36 | | $2a_u$:$4e_g$ | 6 |
| | | | | $a_u$,$2b_{3u}$:$4e_g$ | 5 |
| $2E_u$ | $2a_u$:$4e_g$ | 21 | $4E_u$ | $4b_{1u}$:$4e_g$ | 31 |
| | $6b_{1u}$:$4e_g$ | 21 | | $2a_u$,$2e_g$:$4e_g$ | 12 |
| | $4b_{1u}$:$4e_g$ | 21 | | $6b_{1u}$:$4e_g$ | 7 |
| | $5b_{1u}$:$4e_g$ | 9 | | $2a_u$:$4e_g$ | 7 |

[a]Calculations were made within 6-31+G(d) basis set and active space (14/16).

The studied excited states in $B_{3u}$, $B_{2u}$, $A_g$, and $B_{1g}$ irreps. exhibit basically valence character. However, the $1B_{3g}$, $1B_{2g}$, $1A_u$, and $1B_{1u}$ excited states are of the Rydberg type. This is in agreement with the results of other calculations (CIS and RPA).[38]

*CASSCF, CASPT2.* The CASPT2 approach represents one of the most reliable methods for the electronic spectra calculations, when all valence orbitals can be included in the active space of the CASSCF reference function(s). However, such a large calculation cannot be performed in the case of FBP. All previous CASPT2 studies[27–29] used only very limited active spaces composed on the basis of occupation numbers of nature orbitals in RASSCF calculations. The choice of active orbitals plays a key role in the accuracy of the results.

We studied the effect of basis set augmentation within the recommended active space (14/16). In order to calculate all the lowest spectral lines, an extension of the active space by virtual orbitals from $A_g$, $B_{3u}$, $B_{2u}$, and $B_{1g}$ irreps. is necessary. Using 6-31+G(d) basis set, calculations with even more extended active spaces could not be performed. Active spaces with reduced number of electrons were tested for this purpose, but the quality of the estimated spectral lines was greatly affected.

The composition of CASSCF wave function is depicted in Table 3. Interestingly, the excitations from $3b_{1u}$ orbital play an important role in the lowest visible transitions. Such an influence was not observed in SAC/SAC-CI calculations.

Calculated CASSCF and CASPT2 spectra are summarized in Table 4, where for comparison the results determined within (4/4) active space are also displayed. For the Q and B bands, the calculations performed within (4/4) active space provide an excellent agreement with the experimental data. However, passing to the higher transitions is a much more demanding task. Nevertheless, using the suggested active space, a very good agreement for the higher transitions was also obtained. The calculated transition energies of higher roots only slightly overestimate the experimental values. Our results strongly support traditional assignment of spectral lines, where $1B_{3u}$ + $1B_{2u}$ belong to Q, $2B_{2u}$ + $2B_{3u}$ to B, and $3B_{2u}$ + $3B_{3u}$ to the N spectral bands. The comparison of calculated spectra lines is depicted in Figure 3. As it can be seen, CASPT2 level spectral lines match the experimental spectrum better than the SAC-CI level results, where agreement for only the near-UV part of the spectrum was achieved. The inaccuracy of the first transition energy was already discussed above and is also mentioned in the Conclusion.

Both the SAC-CI and CASPT2 level spectral line intensities show similar characteristics. The predicted intensities of $1B_{3u}$ and $1B_{2u}$ transitions are slightly lower, moreover their ratio is inverted in comparison with the experimental data. On the contrary, the intensity of the B band is slightly higher, and there is worse agreement between experimentally determined N band and the calculated $3B_{3u}$ and $3B_{2u}$ intensities, where both SAC-CI and CASSI level predictions are significantly higher. The discussion on the intensity changes due to close proximity of the excited electronic levels was recently published in Ref. 45.

### *Magnesium Porphin*

#### *Ground State Electronic Structure*

Both the SAC/SAC-CI and CASPT2 level calculations were carried out in $D_{4h}$ symmetry. The ground state of MgP has the following electronic configuration: $22a_g^2$ $18b_{2u}^2$ $18b_{3u}^2$ $14b_{1g}^2$ $6b_{1u}^2$ $3b_{3g}^2$ $3b_{2g}^2$ $2a_u^2$. Due to the higher point group symmetry, MO sets of $b_{2u}$ and $b_{3u}$ orbitals are degenerated in $e_u$ irrep., and similarly,

**Table 4.** CASSCF and CASPT2 Calculated Spectra Lines.[a]

| FBP | $1B_{3u}$ | $2B_{3u}$ | $3B_{3u}$ | $4B_{3u}$ | $1B_{2u}$ | $2B_{2u}$ | $3B_{2u}$ | $4B_{2u}$ |
|---|---|---|---|---|---|---|---|---|
| (4/4) | 4.56 | 7.60 | 12.2 | 14.2 | 4.11 | 5.17 | 12.1 | 14.2 |
| | **1.99** | **3.29** | **6.59** | **6.90** | **2.42** | **3.24** | **6.85** | **6.85** |
| | *0.04* | *1.20* | *0.00* | *0.00* | *0.07* | *1.66* | *0.00* | *0.00* |
| (14/16) | 2.69 | 4.64 | 5.27 | 5.62 | 3.49 | 4.98 | 5.51 | 5.80 |
| | **2.02** | **3.46** | **3.73** | **4.73** | **2.36** | **3.26** | **3.89** | **4.53** |
| | *0.02* | *1.49* | *0.33* | *0.52* | *0.00* | *0.68* | *1.60* | *0.37* |

| MgP | $1E_u$ | $2E_u$ | $3E_u$ | $4E_u$ |
|---|---|---|---|---|
| (4/4) | 3.98 | 5.15 | 12.0 | 14.2 |
| | **2.16** | **3.15** | **6.68** | **6.80** |
| | *0.06* | *1.62* | *0.00* | *0.00* |
| (14/16) | 3.14 | 4.90 | 5.11 | 5.52 |
| | **2.15** | **3.41** | **3.61** | **4.47** |
| | *0.02* | *0.89* | *0.84* | *0.58* |

[a] First lines are CASSCF transition energies, **bold** are PT2 corrected energies (eV), italic are corresponding transition dipole moments (a.u.).

$b_{2g}$ and $b_{3g}$ orbitals in the $e_g$ representation. According to the Hartree-Fock level calculations with the 6-31+G(d) basis set, the HOMO is represented by the $2a_u$ orbital. Lower in energy, there are $6b_{1u}$ and $5b_{1u}$ orbitals, then $3e_g$ and below $4b_{1u}$. The LUMO is represented by the $4e_g$ orbitals. Contrary to FBP, the $23a_g$ and $3a_u$ orbitals are above LUMO here. They are both basically localized on Mg with two diffuse lobes of the same phase in the $23a_g$ orbital and opposite phase in $3a_u$, resembling $3p_z$ Mg AO, but flat and substantially more diffuse.

### *Spectra Calculations of Singlet States*

*SAC/SAC-CI.* The configuration selection thresholds LevelTwo were used for all calculations with the 6-31+G(d) basis set. Comparable thresholds were applied in the only one published SAC-CI study of the MgP spectrum.[22]

The lowest degenerate $E_u$ electronic excitations correspond to the Q band. Their energy is approximately 0.4 eV below the experimentally observed values for MgEthioP[11] and MgTPP[12] (see Table 5 and Fig. 4). The $2E_u$ excitations are assigned to the B band and their transition energy is slightly above experimental value. The 4 orbital transitions occur with contributions approaching the 90 and 85% weights in these two lowest states, giving excellent justification for Gouterman's model. The $3E_u$ excitations are assigned to the N band, and their transition energies are in good agreement with the experimental data. This electronic transition is mainly described by the excitation from $5b_{1u}$ to $4e_g$ orbital (85%).

The lowest excited states in $E_g$, $A_u$ and $B_{1u}$ irreps., display Rydberg character. The corresponding transition energies are about 0.5–1.5 eV lower than the values calculated with the 6-31G basis set (cf. Table 2). This is in good accord with previously performed CIS and RPA level calculations.[38]

*CASSCF, CASPT2.* Similar to FBP, the excitations from $4b_{1u}$ and $5b_{1u}$ orbitals are strongly coupled with the 4 orbital character of $2E_u$ transitions (B-band). The excitation from $5b_{1u}$ to LUMO prevails in the third $E_u$ state where its weight amounts to about 49%. Finally, the excitation from $4b_{1u}$ to LUMO dominates in $4E_u$ transition (31%) (cf. Table 3).

Calculated CASSCF and CASPT2 level electronic spectra are summarized in Table 4. The first transition energy is in very good agreement with the experimental Q band. The second and the third roots could be assigned to the B and N bands, but they differ from the experimental data by 0.2 eV. Moreover, they deviate in opposite directions: overestimating the B band and underestimating the N band. The least certain is the assignment of the 4th root to the weak L band—the value is underestimated by more than 0.3 eV.

Alike in the case of the FBP, SAC-CI and CASSCF level calculated electronic spectral line intensities show similar characteristics. The calculated SAC-CI intensity of B band agrees well with the available experimental data for metallo-porphines. However, the predicted intensities of Q and N bands are too low. The CASSI level estimated intensity of Q band is also too low. The intensity of N band is higher than experimental value at the expense of B band intensity.

### Spectra Estimation with Various Methods

One of the goals of the present study is comparison of selected methods commonly used for predictions of the electronic transitions within the same AO basis set. SAC-CI and CASPT2 level results are compared with the other approximations—CIS, RPA, TDDFT, and semiempirical ZINDO methods. The predicted spectral transitions are collected in Table 5. At the first glance, one notices that neither CIS nor RPA (noncorrelated methods) can be used for more than a rough qualitative estimation. The ZINDO approach managed to fit all the low-laying lines relatively well (including intensities). However, the problems start in N-band region. We conclude that considering the quality of basis sets in semiempirical approximations and consumed CPU time, the re-

**Table 5.** Theoretical and Experimental Spectra Comparison.[a]

| FBP | $1A_g$ | $1B_{3u}$ | $2B_{3u}$ | $3B_{3u}$ | $1B_{2u}$ | $2B_{2u}$ | $3B_{2u}$ | $1B_{1g}$ | $1B_{1u}$ | $1B_{2g}$ | $1B_{3g}$ | $1A_u$ |
|---|---|---|---|---|---|---|---|---|---|---|---|---|
| CIS[b] | **5.56** | **2.46** | **4.57** | **5.42** | **2.57** | **4.73** | | **5.00** | **5.60** | **5.54** | **5.46** | **5.19** |
| | | *0.04* | *1.98* | *1.57* | *0.03* | *2.95* | | | *0.01* | | | |
| RPA[b] | **5.35** | **1.79** | **4.01** | **5.16** | **1.94** | **4.06** | | **4.88** | **5.60** | **5.53** | **5.46** | **5.19** |
| | | *0.03* | *1.35* | *0.46* | *0.02* | *1.54* | | | *0.01* | | | |
| B3LYP[b] | **3.75** | **2.34** | **3.43** | **3.93** | **2.49** | **3.55** | **3.88** | **3.57** | **4.19** | **4.10** | **4.17** | **4.12** |
| | | *0.00* | *0.60* | *0.66* | *0.00* | *0.90* | *0.33* | | *0.00* | | | |
| SAC-CI | **4.41** | **1.80** | **3.57** | **4.23** | **2.13** | **3.67** | **4.34** | **3.71** | **4.70** | **4.83** | **4.77** | **4.59** |
| | | *0.01* | *1.17* | *0.95* | *0.00* | *1.64* | *0.35* | | *0.01* | | | |
| CAS-PT2 | | **2.02** | **3.46** | **3.73** | **2.36** | **3.26** | **3.89** | | | | | |
| | | *0.02* | *1.49* | *0.33* | *0.00* | *0.68* | *1.60* | | | | | |
| ZINDO[b] | **3.68** | **1.75** | **3.50** | **4.22** | **2.08** | **3.61** | **4.62** | **3.82** | **4.48** | **4.43** | **4.39** | **4.53** |
| | | *0.04* | *2.01* | *1.15* | *0.06* | *2.51* | *0.30* | | *0.02* | | | |
| exp.[c] | | **1.98** | **3.33** | **3.65** | **2.42** | **3.33** | **3.65** | | | | | |
| | | *0.01* | *1.15* | *0.10* | *0.06* | *1.15* | *0.10* | | | | | |

| MgP | $1A_g$ | $1E_u$ | $2E_u$ | $3E_u$ | $1B_{1g}$ | $1B_{1u}$ | $1E_g$ | $1A_u$ |
|---|---|---|---|---|---|---|---|---|
| CIS[b] | **4.62** | **2.52** | **4.69** | **5.57** | **5.14** | **4.87** | **4.85** | **4.36** |
| | | *0.04* | *2.78* | *0.23* | | *0.00* | | |
| RPA[b] | **4.62** | **1.89** | **4.06** | **5.42** | **5.14** | **4.86** | **4.85** | **4.36** |
| | | *0.03* | *1.49* | *0.08* | | *0.00* | | |
| B3LYP[b] | **4.10** | **2.47** | **3.60** | **3.96** | **3.93** | **4.63** | **4.60** | |
| | | *0.00* | *1.03* | *0.03* | | *0.00* | | |
| SAC-CI | **4.09** | **1.68** | **3.29** | **3.81** | **3.94** | **3.82** | **4.14** | **3.66** |
| | | *0.01* | *1.56* | *0.00* | | *0.00* | | |
| CAS-PT2 | | **2.15** | **3.41** | **3.61** | | | | |
| | | *0.02* | *0.89* | *0.84* | | | | |
| ZINDO[b] | **4.81** | **1.97** | **3.63** | **4.50** | **4.24** | | **4.59** | **3.65** |
| | | *0.07* | *2.59* | *0.07* | | | | |
| exp. MgEthioP[d] | | **2.14** | **3.18** | **3.82** | | | | |
| exp. MgTPP[c] | | **2.07** | **3.04** | **3.96** | | | | |
| exp.[d] | | *0.1* | *1.1–1.6* | *0.1* | | | | |

[a] **Bold** are transition energies (eV), italic are corresponding transition dipole moments (a.u.). 6-31+G(d) basis set was used.

[b] Ref. 38.

[c] Ref. 12.

[d] Ref. 11.

sults are very satisfactory. One has to be aware that the ZINDO method has to be used with caution and the correct order of MOs must be checked. Otherwise, qualitatively wrong spectral lines can appear, as was noticed by our study on the pheophytine spectrum (not published).

Also, several DFT functionals were tested in TDDFT calculations: B3LYP, B3PW91, and BP86. Based on the RMS values, the best B3LYP data were chosen for presentation in Table 5. We believe that some of the deviations of B3LYP spectrum lines origin from "inconsistent" reference geometry because the molecular structure optimization was performed at the HF/6-31G(d) level (cf. ref. 38).

### *Comparison with Recent Calculations*

In Tables 6 and 7 selected recent calculations on both molecules are collected. For the correlated calculations, double-zeta (DZ) basis set quality seems to be sufficient for a reasonable agreement with the experimental spectra. Larger basis sets calculations are less frequent because of high computational demands due to the relatively large size of the studied systems.

As can be seen from the results of Table 6, the values obtained at the STEOM-CC[23] and SAC-CI[19] levels are quite similar. More detailed consideration of the role of the polarization and diffuse functions reveals only small differences between these two levels of theory. Surprisingly, the results published by Kitao[21] with 4-31+G(d) basis set do not provide any improvement in comparison with Tokita's DZ(d)/DZ+ level calculations.[20] The one common feature apparent from Table 6 and 7 is that while both the methods underestimate the lowest Q transitions, the other spectral lines exhibit systematical blue shift. Similar trends can also be noticed from Table 5 for RPA and semiempirical ZINDO methods.

Our CASPT2 results well match the results of calculations previously published by Merchan and Roos.[29] Preserving the selection of the active space, the effect of a more flexible AO basis set led to substantial improvement of the estimated electron transitions, when compared with measured spectra lines.

Several other calculations using multireference CI approach were also recently published. Three of them[25,30,36] are mentioned in Table 6 and one can conclude that a careful selection of the considered reference space leads to a very accurate spectra prediction. However, the first two mentioned studies limit their attention only to the lowest transitions from the visible part of the spectrum.

As it has been noted in the literature many times, the TDDFT method represents a very successful and relatively cheap approach to making accurate spectra predictions. In Table 6 van Gisbergen's data using the ALDA functional are presented.[33] They are in accord with our results obtained using BP86 functional and also with the results published by Sundholm using Becke-Perdew functional.[34] All higher lying transitions from these studies exhibit red-shift, which somehow contradicts calculations using B3LYP or B3PW91 functionals (cf. Table 5), where better correspondence with experimental data (usually slightly blue-shifted, cf. ref. 35,38) is observed. Also, the results from other calculations (not related to studied molecules) indicate the same trend and this is generally explained by the wrong limits (going to higher excited states) of the density functionals. Therefore the performance of the ALDA and BP86 functionals represents an interesting case.

Another challenge concerns a proper estimation of the spectral line intensities. While usually the intensities of the two lowest transitions agree reasonably well, the third line is predicted with substantially higher intensity by all the investigated methods. The TDDFT methods fail in intensity predictions also for the 2nd transition in $B_{3u}$ irrep too.

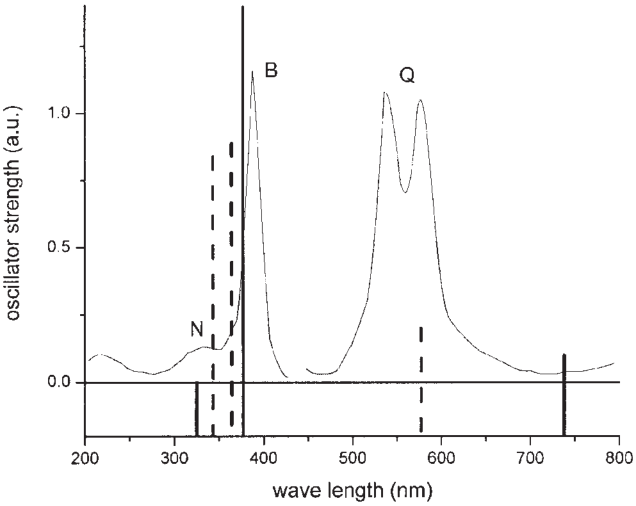

**Figure 4.** Comparison of calculated spectra of MgP with experimental data determined on MgEthioP.[11] Solid lines represent SAC-CI determined transitions, dashed lines correspond to CASPT2 spectrum. Q band intensity is 10× enlarged. Thanks to higher symmetry, there is only one degenerate band in the Q band region of the MgP spectrum.

**Table 6.** Spectra Transitions Published in Literature Recently for FBP.

| | $1B_{3u}$ | $2B_{3u}$ | $3B_{3u}$ | $1B_{2u}$ | $2B_{2u}$ | $3B_{2u}$ |
|---|---|---|---|---|---|---|
| MRSDspCI/DZ+[a] | **1.97** | **3.41** | | **2.40** | **3.24** | |
| CIS/6-31+G[b] | **2.53** | **4.60** | | **2.66** | **4.80** | |
| CASPT2/DZ[c] | **1.70** | **2.91** | | **2.26** | **3.04** | |
| | *0.00* | *1.66* | | *0.02* | *1.54* | |
| CASPT2/DZ*[d] | **1.63** | **3.08** | **3.42** | **2.11** | **3.12** | **3.53** |
| | *0.00* | *0.91* | *0.46* | *0.00* | *0.70* | *0.83* |
| STEOM-CC/DZ[e] | **1.72** | **3.66** | **4.28** | **2.61** | **3.77** | **4.67** |
| | — | *1.03* | *0.71* | *0.02* | *1.42* | *0.44* |
| STEOM-CC/DZ*[f] | **1.75** | **3.47** | **4.06** | **2.40** | **3.62** | **4.35** |
| | *0.00* | *0.69* | *0.93* | *0.01* | *1.20* | *0.42* |
| STEOM-CC/DZ+[f] | **1.70** | **3.63** | **4.22** | **2.59** | **3.74** | **4.63** |
| | — | *0.98* | *0.74* | *0.02* | *1.37* | *0.44* |
| SAC-CI/DZ[g] | **1.75** | **3.56** | **4.24** | **2.23** | **3.75** | **4.52** |
| | *0.00* | *1.00* | *1.00* | *0.01* | *1.70* | *0.40* |
| SAC-CI/DZ*[h] | **1.77** | **3.47** | **4.20** | **2.01** | **3.73** | **4.38** |
| | *0.00* | *0.77* | *1.32* | *0.01* | *1.62* | *0.34* |
| SAC-CI/DZ+[h] | **1.70** | **3.43** | **4.08** | **2.19** | **3.62** | **4.36** |
| | *0.00* | *1.10* | *1.09* | *0.01* | *1.87* | *0.44* |
| SAC-CI/4-31+G*[i] | **1.81** | **3.47** | **4.23** | **2.10** | **3.69** | **4.40** |
| | *0.00* | *0.90* | *1.63* | *0.02* | *1.88* | *0.58* |
| TDDFT (ALDA)[j] | **2.16** | **3.01** | **3.41** | **2.29** | **2.98** | **3.47** |
| | *0.01* | *0.04* | *0.90* | *0.00* | *0.13* | *0.73* |
| TDDFT (B3LYP)[k] | **2.24** | **3.27** | **3.79** | **2.39** | **3.45** | **3.70** |
| | *0.00* | *0.40* | *0.82* | *0.00* | *0.61* | *0.55* |
| MRMP[l] | **1.63** | **3.10** | | **2.55** | **3.25** | |
| | *0.00* | *1.61* | | *0.01* | *1.53* | |
| DFT/MRCI[m] | **1.94** | **3.07** | **3.79** | **2.38** | **3.17** | **3.70** |
| | *0.00* | *0.48* | *0.82* | *0.00* | *0.66* | *0.55* |
| exp.[n] | **1.98** | **3.33** | **3.65** | **2.42** | **3.33** | **3.65** |
| | *0.01* | *1.15* | *0.10* | *0.06* | *1.15* | *0.10* |

[a] Ref. 25.
[b] Ref. 15.
[c] Ref. 27.
[d] Ref. 28.
[e] Ref. 23.
[f] Ref. 24.
[g] Ref. 19.
[h] Ref. 20.
[i] Ref. 21.
[j] Ref. 33.
[k] Ref. 35.
[l] Ref. 30.
[m] Ref. 36.
[n] Ref. 12.

## Conclusions

- Electronic absorption spectra of the FBP and MgP molecules were calculated using SAC/SAC-CI and CASPT2 methods. The results of these calculations were compared with the previously published CIS, RPA, CASSCF, TD-DFT, and ZINDO level spectral studies. An extended 6-31+G(d) basis set was used for a qualitatively acceptable description of the investigated spectra.
- The lowest calculated pair of transitions (1B3u and 1B2u)

**Table 7.** Spectra Transitions Recently Published for MgP.

| | $1E_u$ | $2E_u$ | $3E_u$ |
|---|---|---|---|
| SAC-CI/DZ*[a] | **2.01** | **3.63** | **4.15** |
| | *0.002* | *1.99* | *0.07* |
| CASPT2/DZ*[b] | **1.66** | **2.66** | **3.11** |
| | *0.04* | *0.82* | *0.15* |
| MRMP[c] | **2.00** | **3.07** | |
| | 0.011 | 1.561 | |
| TDDFT[d] | **2.21** | **3.15** | **3.25** |
| | 1E-04 | *0.06* | *0.58* |
| DFT/MRCI[e] | **2.16** | **3.25** | **3.63** |
| | *0.002* | *1.27* | *0.034* |
| exp. MgEthioP[f] | **2.14** | **3.18** | **3.82** |
| exp. MgTPP[g] | **2.07** | **3.04** | **3.96** |
| exp.[f] | *0.1* | *1.1–1.6* | *0.1* |

[a] Ref. 22.
[b] Ref. 29.
[c] Ref. 30.
[d] Ref. 35.
[e] Ref. 36.
[f] Ref. 11.
[g] Ref. 12.

of FBP corresponds to the $Q_x$ and $Q_y$ bands. The next two pairs are assigned to B and N bands, respectively.

- The SAC-CI level spectrum of FBP is in very good agreement with the experimental data. The lowest ($1B_{3u}$) line is by ~0.2 eV underestimated, similar to the results of previously carried out RPA and ZINDO calculations. However, the third roots in both $B_{3u}$ and $B_{2u}$ symmetry, assigned to N band, are by ~0.6 eV overestimated. The higher correlation effects should be included for the quantitative correspondence with the experimental data.
- The configuration selection thresholds used in previously published articles limit the accuracy of obtained spectra, as was demonstrated by SAC-CI/6-31G level calculations. Further non-negligible improvement was achieved, when five times more accurate thresholds were used. For very accurate estimation of electron spectra at SAC-CI level, a higher level of thresholds would probably need to be employed, which is impossible for such large molecules at present.
- For the FBP molecule, the $A_u$, $B_{1u}$, $B_{2g}$, and $B_{3g}$ symmetry lowest excited states exhibit Rydberg character. The other transitions ($A_g$, $B_{1g}$, $B_{2u}$, and $B_{3u}$ symmetry) represent the valence type. Nevertheless, in the MgP case the lowest $A_g$ and $B_{1g}$ transitions also represent the Rydberg type.
- The FBP and MgP spectral lines were reproduced with high accuracy using the CASPT2 approximation.
- For a correct description of the complete set of spectral lines, it is also important to extend the active space by addition of at least selected virtual MOs from irreps. $A_g$, $B_{2u}$, $B_{3u}$, and $B_{1g}$ irreps. However, such an extension is extremely computationally demanding. It also can be achieved at the expense of visible spectrum quality.
- Both the CASPT2 and SAC/SAC-CI level calculations are approaching the current limits for accurate calculations of porphin derivates' electronic spectra using high-performance supercomputers.

## Acknowledgments

The authors thank Prof. J. Hala from the Charles University and Prof. F. Vacha from University of South Bohemian in České Budějovice for fruitful and helpful discussions and kind access to their computational facilities. Generous computational support was provided by the Computational Centers of Charles University in Prague, Prague's Technical University, Masaryk University in Brno, West Bohemia University in Pilsen, and the Mississippi Supercomputer Center in Oxford, MS.

## References

1. Gouterman, M. The Porphyrins, Vol. 3; Academic Press: New York, 1977.
2. Akimoto, S.; Yamazaki, T.; Yamazaki, I.; Osuka, A. Chem Phys Lett 1999, 309, 177.
3. Almlof, J.; Fischer, T. H.; Gassman, P. G.; Ghosh, A.; Haser, M. J Phys Chem 1993, 97, 10964.
4. Asano-Someda, M.; Ichino, T.; Kaizu, Y. J Phys Chem A 1997, 101, 4484.
5. Behar, D.; Dhanasekaran, T.; Neta, P. J Phys Chem A 1998, 102, 2870.
6. Gurzadyan, G. G.; Tran-Thi, T.-H.; Gustavsson, T. J Chem Phys 1998, 108, 385.
7. Linnanto, J.; Korppi-Tommola, J Phys Chem Chem Phys 2000, 2, 4962.
8. Vitols, S. E.; Kumble, R.; Blackwood Jr., M. E.; Roman, J. S.; Spiro, T. G. J Phys Chem 1996, 100, 4180.
9. Yu, H. Z.; Baskin, J. S.; Steiger, B.; Wan, C. Z.; Anson, F. C.; Zewail, A. H. Chem Phys Lett 1998, 293, 1.
10. Zerner, M. G. Theor Chim Acta 1966, 4, 44.
11. Edwards, L.; Dolphin, D. H.; Gouterman, M. J Mol Spectrosc 1970, 35, 90.
12. Edwards, L.; Dolphin, D. H.; Gouterman, M.; Adler, A. D. J Mol Spectrosc 1971, 38, 16.
13. Gouterman, M. J Chem Phys 1959, 30, 1139.
14. Gouterman, M.; Wagniere, G. H. J Mol Spectrosc 1963, 11, 108.
15. Foresman, J. B.; Head-Gordon, M.; Pople, J. A.; Frisch, M. J. J Phys Chem 1992, 96, 135.
16. Nakatsuji, H.; Hirao, K. J Chem Phys 1978, 68, 2035.
17. Nakatsuji, H. Chem Phys Lett 1978, 59, 362.
18. Nakatsuji, H. Chem Phys Lett 1979, 67, 329.
19. Nakatsuji, H.; Hasegawa, J.-y.; Hada, M. J Chem Phys 1996, 104, 2321.
20. Tokita, Y.; Hasegawa, J.; Nakatsuji, H. J Phys Chem A 1998, 102, 1843.
21. Kitao, O.; Ushiyama, H.; Miura, N. J Chem Phys 1999, 110, 2936.
22. Hasegawa, J.; Hada, M.; Nonoguchi, M.; Nakatsuji, H. Chem Phys Lett 1996, 250, 159.
23. Nooijen, M.; Bartlett, R. J. J Chem Phys 1997, 107, 6812.

24. Gwaltney, S. R.; Bartlett, R. J. J Chem Phys 1998, 108, 6790.
25. Yamamoto, Y.; Noro, T.; Ohno, K. Int J Quantum Chem 1992, 42, 1563.
26. Celani, P.; Werner, H. J Chem Phys 2000, 112, 5546.
27. Merchan, M.; Orti, E.; Roos, B. Chem Phys Lett 1994, 226, 27.
28. Serrano-Andres, L.; Merchan, M.; Rubio, M.; Roos, B. O. Chem Phys Lett 1998, 295, 195.
29. Rubio, M.; Roos, B.; Serrano-Andres, L.; Merchan, M. J Chem Phys 1999, 110, 7202.
30. Hashimoto, T.; Choe, E.; Nakano, H.; Hirao, K. J Phys Chem A 1999, 103, 1894.
31. Bauernschmitt, R.; Ahlrichs, R. Chem Phys Lett 1996, 256, 454.
32. Stratmann, R.; Scuseria, G.; Frisch, M. J Chem Phys 1998, 109, 8218.
33. van Gisbergen, S.; Rosa, A.; Ricciardi, G.; Baerends, E. J Chem Phys 1999, 111, 2499.
34. Sundholm, D. Phys Chem Chem Phys 2000, 2, 2275.
35. Sundholm, D. Chem Phys Lett 2000, 317, 392.
36. Parusel, A.; Grime, S. J Prophyr Phthalocyanines 2001, 5, 225.
37. Parusel, A. B. J.; Grimme, S. J Phys Chem B 2000, 104, 5395.
38. Burda, J. V.; Šeda, J.; Brázdová, V.; Kapsa, V. Int J Mol Sci 2004, 5, 196.
39. Lamoen, D.; Parrinello, M. Chem Phys Lett 1996, 248, 309.
40. Merchan, M.; Orti, E.; Roos, B. Chem Phys Lett 1994, 221, 136.
41. Hariharan, P. C.; Pople, J. A. Theor Chim Acta 1973, 28, 213.
42. Clark, T.; Chandrasekhar, J.; Schleyer, P. V. R. J Comput Chem 1983, 4, 294.
43. Frisch, M. J.; Trucks, G. W.; Schlegel, H. B.; Scuseria, G. E.; Robb, M. A.; Cheeseman, J. R.; Montgomery, J. A.; Vreven, J. T.; Kudin, K. N.; Burant, J. C.; Millam, J. M.; Iyengar, S. S.; Tomasi, J.; Barone, V.; Mennucci, B.; Cossi, M.; Scalmani, G.; Rega, N.; Petersson, G. A.; Nakatsuji, H.; Hada, M.; Ehara, M.; Toyota, K.; Fukuda, R.; Hasegawa, J.; Ishida, M.; Nakajima, T.; Honda, Y.; Kitao, O.; Nakai, H.; Klene, M.; Li, X.; Knox, J. E.; Hratchian, H. P.; Cross, J. B.; Adamo, C.; Jaramillo, J.; Gomperts, R.; Stratmann, R. E.; Yazyev, O.; Austin, A. J.; Cammi, R.; Pomelli, C.; Ochterski, J. W.; Ayala, P. Y.; Morokuma, K.; Voth, G. A.; Salvador, P.; Dannenberg, J. J.; Zakrzewski, V. G.; Dapprich, S.; Daniels, A. D.; Strain, M. C.; Farkas, O.; Malick, D. K.; Rabuck, A. D.; Raghavachari, K.; Foresman, J. B.; Ortiz, J. V.; Cui, Q.; Baboul, A. G.; Clifford, S.; Cioslowski, J.; Stefanov, B. B.; Liu, H.; Liashenko, A.; Piskorz, P.; Komaromi, I.; Martin, R. L.; Fox, D. J.; Keith, T.; Al-Laham, M. A.; Peng, C. Y.; Nanayakkara, A.; Challacombe, M.; Gill, P. M. W.; Johnson, B.; Chen, W.; Wong, M. W.; Gonzalez, C.; Pople, J. A. GAUSSIAN 03, Revision A.1; Gaussian, Inc.: Pittsburgh, PA, 2003.
44. Karlström, G.; Lindh, R.; Malmqvist, P.-Å.; Roos, B. O.; Ryde, U.; Veryazov, V.; Widmark, P.-O.; Cossi, M.; Schimmelpfennig, B.; Neogrady, P.; Seijo, L. Comput Material Sci 2003, 28, 222.
45. Stanton, J. F.; Sattelmeyer, K. W.; Gauss, J.; Allan, M.; Skalicky, T.; Bally, T. J Chem Phys 2001, 115, 1.